Дистанционное зондирование сред

УДК 621.396

ПОЛЯРИЗАЦИОННЫЕ РАДАРНЫЕ МЕТОДЫ ИЗМЕРЕНИЯ СНЕЖНЫХ ОСАДКОВ

Петар Буковчич
PhD, научный сотрудник Кооперативного института мезомасштабных метеорологических исследований[1], университета Оклахомы[2] и Национальной лаборатории по исследованию сильных штормов[3].
E-mail: Petar.Bukovcic@noaa.gov

Рыжков Александр Васильевич
кандидат физико-математических наук, адьюнкт-профессор университета Оклахомы[2], старший научный сотрудник Национальной лаборатории по исследованию сильных штормов[3].
E-mail: Alexander.Ryzhkov@noaa.gov

[1, 2, 3] *Адрес:* 120 David L Boren Blvd., Norman, Oklahoma, USA, 73072.

Аннотация: В своем недавнем исследовании Буковчич и др. использовали большой массив данных по измерению снежных осадков, полученный с помощью двумерного видео-дисдрометра в центральной Оклахоме для вывода уравнений по определению интенсивности снежных осадков S. Эти уравнения содержат удельную дифференциальную фазу K_{DP} и радарную отражаемость Z и имеют вид $S(K_{DP}, Z) = \gamma K_{DP}^{\alpha} Z^{\beta}$. Анализ уравнений показывает, что фактор γ в определённой степени зависит от изменений формы и ориентации снежинок, в то время как коэффициенты α и β практически инвариантны по отношению к этим изменениям. Поляризационные формулы для определения снежных осадков были использованы при анализе радарных данных, полученных в разных географических регионах США: Оклахоме, Вирджинии и Колорадо. Применение поляризационных методик продемонстрировало существенное улучшение оценок снежных осадков по сравнению с традиционными Z – методами, что является обнадеживающим результатом.

Ключевые слова: измерения снежных осадков, поляриметрические соотношения, ширина спектра, поляризационные радарные методы, улучшенные вертикальные профили.

1. Introduction

Accurate radar measurements of snow are very challenging and difficult to accomplish. There is a high degree of natural variability in particle size distributions (PSD), snowflake densities, shapes, orientations, water contents, and habits, which increases the level of complexity in remote snow measurements. Historically, the equivalent reflectivity factor at horizontal polarization (Z_h) has been used for snow water-equivalent rates (S) estimation, typically in the form of power-law relations where Z is proportional to S^2 (e.g., Gunn and Marshall [1]; Sekhon and Srivastava [2]; Fujiyoshi et al., [3]; Matrosov et al., [4, 5]; Szyrmer and Zawadzki [6]; Zhang et al., [7]; Heymsfield et al., [8]; etc.). Because the Z-based relations are sensitive to natural PSD variability and change in particle density, the difference between existing $S(Z)$ estimates is large about an order of magnitude for a given value of Z.

Dual-polarization radars provide additional independent information about the hydrometeor characteristics. Recent polarimetric upgrade of the National Weather Service WSR-88D radar network in the US offers unique opportunity to improve the accuracy of precipitation measurements including snow quantification. However, even with the plethora of polarimetric measurements at our disposal the wealth of polarimetric radar information is still underutilized. Indeed, after three

decades of polarimeric research there has been only limited usage of polarimetric information for quantification of ice and snow, mainly for ice water content (IWC) estimation (Vivekanandan et al., [9]; Aydin and Tang [10]; Ryzhkov et al., [11, 12]; Lu et al., [13]; Nguyen et al., [14, 15]). Just recently, Bukovčić et al. [16] derived polarimetric radar relations for snow estimation (applicable at S, C, and X bands) from a large set of video disdrometer (2DVD) data for dry aggregated snow in Oklahoma and Colorado. They introduced a bivariate power-law relation for snow water-equivalent rate estimation based on the specific differential phase K_{DP} and reflectivity factor Z. The novel polarimetric $S(K_{DP}, Z)$ relation has relatively small standard deviation with respect to 2DVD estimates, in sharp contrast with a very large one from $S(Z)$. On the negative side, $S(K_{DP}, Z)$ is very sensitive to the variability of particle density, aspect ratio, and the width of the particle canting angle distribution. Bukovčić et al. [16] tested the $S(K_{DP}, Z)$ relation using simulations of radar variables from the 2DVD data in several geographical locations, and demonstrated encouraging results for snow quantification. For more information about the theoretical background, derivation, and verification of polarimetric relations for snow quantification using 2DVD measurements and computations, the reader is referred to Bukovčić et al., [16] and Ryzhkov and Zrnic [17].

The focus of this paper, an extension of the Bukovčić et al., [16] study, is to test the viability of the novel approach for polarimetric snow estimation through the application to polarimetric radar data. The 2DVD-derived $S(K_{DP}, Z)$ relation is applied to the WSR-88D radar data in three geographical locations, Virginia, Oklahoma, and Colorado and the results are compared to the standard $S(Z)$ estimates and ground (in situ) measurements.

The sensitivity of the $S(K_{DP}, Z)$ polarimetric relation to the variability of the particle shapes and orientations is discussed in section 2, whereas the methodology of radar measurements is presented in section 3. Section 4 contains verification of polarimetric snow relations for three snow cases followed by discussion and summary at the end.

2. Sensitivity of the S(K_{DP}, Z) relation to the variability of particle's aspect ratio b/a and the width of the canting angle distribution σ

It is shown in Bukovčić et al., [16] how the multiplier γ and exponents α and β of the power-law $S(K_{DP}, Z) = \gamma K_{DP}^{\alpha} Z^{\beta}$ relation depend on the particle density, aspect ratio, and the width of the canting angle distribution. The biggest uncertainty comes from σ and b/a, whereas the change in the degree of riming (or snow density) is partially accounted for by the (density) adjustment through the ratio of squares of measured and prescribed empirical velocities (eq. 7 in Bukovčić et al., [16]). The dependences of α, β, and γ on the joint influence of σ and b/a from 2DVD measurements and simulations are illustrated in Fig. 1. The rugged shapes of the curves in Fig. 1a,b are the consequence of the polarimetric relations exponents' discretization

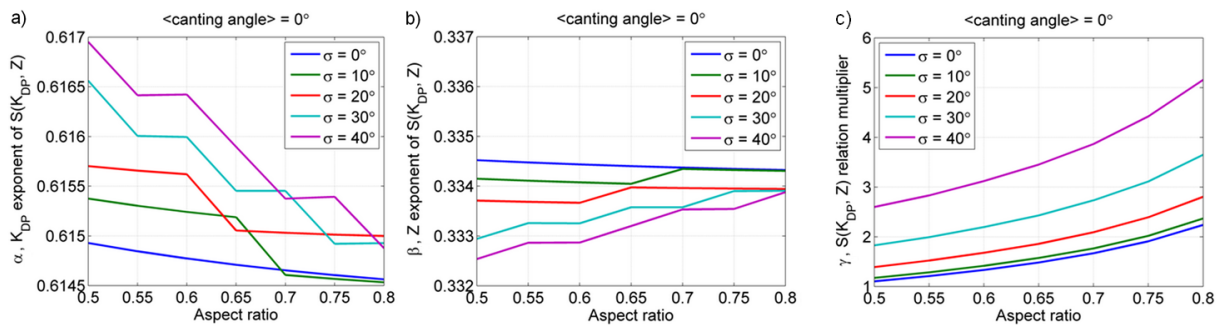

Figure 1. Dependence of the $S(K_{DP}, Z)$ relation's a) K_{DP} exponent α, b) Z exponent β, and c) multiplier γ, on σ and b/a, computed from 2DVD measurements.

in an iterative procedure used to obtain exponents' optimal values.

Both K_{DP} and Z exponents from the $S(K_{DP}, Z)$ relation, α and β, are almost constant (decrease very little) as σ and b/a simultaneously increase (Fig. 1a, b). The largest change in α and β is 0.3% and 0.4% for $\sigma = 40°$ and the increase in b/a from 0.5 to 0.8, which implies that α and β can be regarded as invariant to the changes in σ and b/a. The dependence of the multiplier γ on σ and b/a is dramatically different, as presented in Fig. 1c. For constant σ, and b/a between 0.5 and 0.8, the $S(K_{DP}, Z)$ multiplier γ can increase by a factor of 2. The increase in γ is ~3.5 times if σ and b/a simultaneously increase from 0° to 40° and 0.5 to 0.7 (characteristic values for aggregated snow, Korolev and Isaac 2003), which makes a significant variability in the $S(K_{DP}, Z)$ estimates.

3. Radar data processing

Polarimetric radar measurements contain a wealth of information regarding the precipitating environment, but not all measurements are equally useful. For example, specific differential phase, K_{DP}, is a range derivative of differential phase Φ_{DP} and can be very noisy, especially in snow. Also, the values of K_{DP} are close to zero for irregular-shaped ice particles or aggregated snowflakes. The emergence of new radar data displaying/processing techniques, such as Enhanced (or more appropriate "Columnar") Vertical Profiles (EVPs, Bukovčič et al., [18]) or Quasi Vertical Profiles (QVPs, Ryzhkov et al., [19], Griffin et al., [20]), can help in reduction of the K_{DP} measurement/estimation errors. The QVP product is radar-centric and requires 360° azimuthal averaging. For each radial increment (range gate) within the higher tilt volume scan (usually between 10° and 20°), 360° azimuthal averaged value is projected to the radar centered vertical axis. This gives a QVP for a given radar scan. Repeating this procedure for all available radar volume scans, QVP is a time vs. height format is obtained.

Specifically, the QVP of K_{DP} is obtained as follows. Estimates of Φ_{DP} radial profiles are smoothed and least square fits of a slope at consecutive range locations provide the K_{DP} slant radial profiles. The QVP of K_{DP} is then constructed by azimuthally averaging these profiles to further reduce the statistical errors. Hence, the QVP methodology significantly reduces the noise and improves the accuracy of K_{DP} estimate, decreasing the measurement error to about 0.01 deg km^{-1} (i.e, reducing the standard deviation of the K_{DP} measurement by a factor of $360^{1/2} \approx 19$). This is more than sufficient for K_{DP} to be used in snow estimation in proximity of the radar. The QVPs, presented in time vs. height format, are the essential data for verification of polarimetric snow relations in this study. For a detailed description of the QVP methodology, the reader is referred to Ryzhkov et al., [19].

Another dependency to be accounted for while using the QVP for snow estimation is the variation of particle's aspect ratio as a function of the radar elevation angle (Fig. 2).

For example, if the aspect ratio equals 0.6 at 0° radar elevation angle, its apparent value at 20° elevation would be ~0.645, as depicted in Fig. 2.

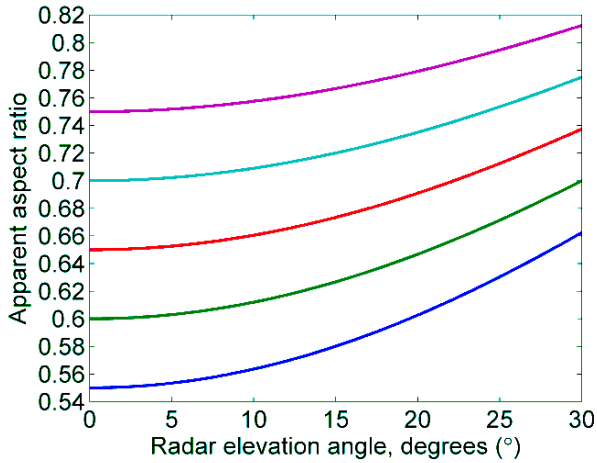

Figure 2. Dependence of the particle's aspect ratio on the radar elevation angle (for σ = 0° and <canting angle> = 0°, where symbol < > represent mean). Blue, green, red, cyan, and magenta lines represent the change in the apparent aspect ratio $(b/a)_\theta$ = 0.55, 0.6, 0.65, 0.7, and 0.75 for different radar elevation angles, from 0° to 30°.

The relation for the aspect ratio dependence on the radar elevation is:

$$(b/a)_\theta = (b/a)_0 \sin^2(90^\circ - \theta) + \cos^2(90^\circ - \theta) = \\ = (b/a)_0 \cos^2\theta + \sin^2\theta, \quad (1)$$

where b/a is the particle's aspect ratio and θ is the radar elevation angle in degrees (subscripts $_\theta$ and $_0$ represent elevation angles θ and 0° respectively, where $(b/a)_\theta$ is the apparent aspect ratio). This means that the multiplier in $S(K_{DP}, Z)$ relation needs to be adjusted for the radar elevation angle according to the Eq. (1) because it has been derived for 0° elevation angle.

4. Verification of the polarimetric radar relations for snow using polarimetric radar data

Three cases from different geographical locations, Virginia, Oklahoma, and Colorado were selected for validation of the $S(K_{DP}, Z)$ polarimetric radar relation. The radar measurements are obtained in dry (mostly) aggregated snow, with one high (~55 mm), and two medium (~15 mm and ~23 mm) total snow water equivalent (SWE) accumulations. The Oklahoma $S_{OK}(K_{DP}, Z) = 1.48K_{DP}^{0.615}Z^{0.33}$ relation from Bukovčić et al., [16] and QVP methodology is used for verification in the first two cases (herein $S_{OK}(K_{DP}, Z)$ is denoted as $S(K_{DP}, Z)$). The Plan Position Indicator (PPI) data and Colorado relation from Bukovčić et al., [16], $S_{CO}(K_{DP}, Z) = 1.88K_{DP}^{0.615}Z^{0.33}$ is used in the Colorado dataset.

a. 23 January 2016 east coast blizzard case, Sterling, VA

The first snowstorm used for verification, 23 January 2016 east coast blizzard, produced about 55 mm of snow water equivalent in 24 hours. The storm hampered the day's activities and services from New York to Washington DC area, affecting an immense number of people. The maps of total snow water equivalent obtained by using the standard $S(Z)$ relation on several WSR-88D radars (not shown) were unsatisfactory in comparison to the heated gauge total accumulation. Also, some heated rain gauges showed much smaller amounts of precipitation due to partially melted or windblown snow. It is well known that widely used $S(Z)$ relations are notoriously inaccurate because of inadequate representation of the variability in snow PSDs. The inclusion of K_{DP} in $S(K_{DP}, Z)$ relation may be a partial remedy for the inadequate snow PSD variability that affects the $S(Z)$ (but only if σ and b/a are a priory known). The KLWX QVPs (19.5° elevation angle) of Z, K_{DP}, Z_{DR}, and $S(K_{DP}, Z)$ in a time vs. height format are presented in Fig. 3. The black dashed lines are isotherms estimated from Rapid Refresh (RAP) model, where the dendritic growth layer (DGL) from -10°C to -20°C is highlighted in magenta.

There are some very informative features visible in QVPs of K_{DP} and Z_{DR} within the DGL including the midlevel maxima in both of these variables. The K_{DP} maxima are associated with the higher ice particle concentration (K_{DP} is usually very low in aggregated snow close to the ground). It is known that in the DGL (temperature range from -10°C to -20°C) dendrites and plates have the strongest growth (hence DGL – dendritic growth layer) at the expense of the water vapor. About 80% – 90% of total precipitation is formed in this layer, which, as seen from the QVPs of K_{DP} and Z_{DR}, has some pronounced signatures. This is mainly because of non-sphericity in ice particles shapes and higher density of particles in the DGL aloft. Further below the DGL aggregation occurs, which decreases the density of the snow particles and redistributes the mass from smaller to the larger sizes. Close to the ground, both K_{DP} and Z_{DR} are near zero due to more spherical shapes of the aggregates, their more chaotic orientation, and low particles' densities. Moreover, the fact that Z_{DR} is close to 0 dB in heavily aggregated snow is used for absolute calibration of Z_{DR} using such snow type (Ryzhkov et al., [21]).

$S(K_{DP}, Z)$ is almost constant from the bottom of the DGL to the ground; ideally a constant values are expected if the mass flux is conserved through this portion of the atmosphere. Often, Z and K_{DP} complement each other in the vertical column. Reflectivity is rather low in DGL whereas K_{DP} is high. It is opposite below the DGL towards the

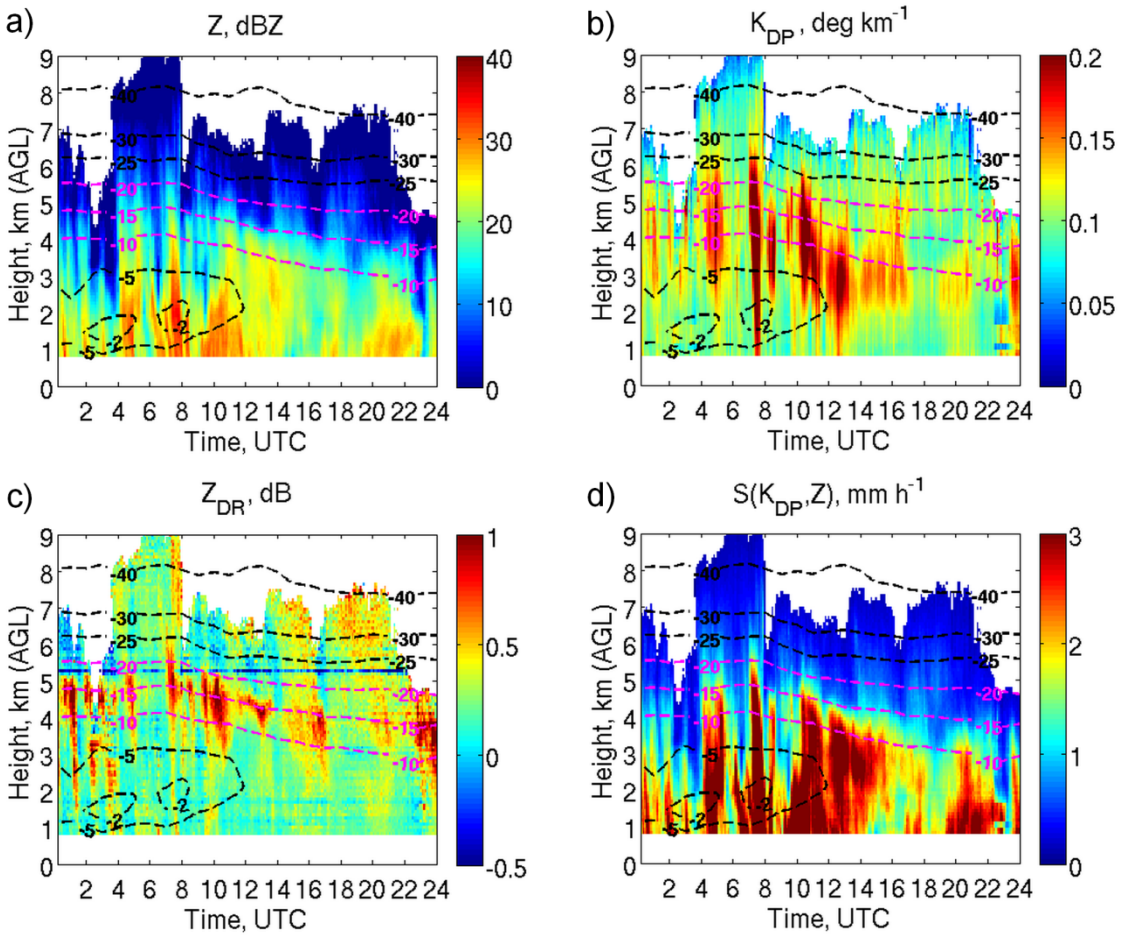

Figure 3. QVPs of a) Z in dBZ, b) K_{DP} in deg km^{-1}, c) Z_{DR} in dB, and d) $S(K_{DP}, Z)$ in mm h^{-1}, KLWX 19.5° radar elevation angle, Sterling VA, 23 January 2016. The black dashed lines are isotherms, where the layer from –10°C to –20°C highlighted in magenta represents DGL.

ground where Z is increasing due to increased particle sizes in aggregated snow and K_{DP} decreases because of particles' increased sphericity and reduction in particles' concentration and aggregates' density.

Verification of the novel polarimetric snow measurement concept is presented in Fig. 4 through the comparisons of $S(K_{DP}, Z)$ relations with collocated reference ground measurements and several $S(Z)$ standard WSR-88D relations. The vertical profiles of total snow accumulations (Fig. 4) are obtained via multiplying $S(Z)$ and $S(K_{DP}, Z)$ relations by the time interval between the radar scans, and at the constant heights, summing the corresponding results throughout the duration of the storm. Both $S(K_{DP}, Z)$ relations used for comparison provide better estimates of total SWE than corresponding $S(Z)$ relations. The two $S(K_{DP}, Z)$ relations are derived for different aspect ratios and radar elevation angles. The red line corresponds to 0° radar elevation and particle aspect ratio 0.65 (the Oklahoma $S(K_{DP}, Z)$ relation), whereas magenta line is derived for 0° elevation and b/a = 0.55, but adjusted for 19.5° radar elevation angle. Note that with increasing radar elevation angle, particle aspect ratio changes via eq. (1), and should be taken into account. In this case b/a = 0.55 aspect ratio at 0° radar elevation becomes apparent aspect ratio $(b/a)_\theta$ = 0.6 at 19.5°, as shown in Fig. 4. Then for practical use, the multiplier γ of the $S(K_{DP}, Z)$ relation for b/a = 0.6 can be estimated from Fig. 1c and used for

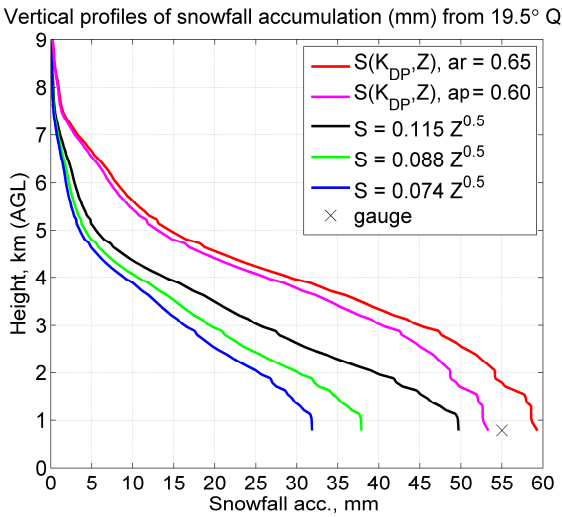

Figure 4. Vertical profiles of total snow accumulation obtained from KLWX 19.5° QVPs using various $S(Z)$s and $S(K_{DP}, Z)$ relations (red: aspect ratio — ar = $(b/a)_{0°}$ = 0.65, magenta: apparent aspect ratio — ap = $(b/a)_{19.5°}$ = 0.6, obtained from $(b/a)_{0°}$ = 0.55 via eq. 1) for 23 January 2016. The X represents reference ground measurements of snow liquid-water equivalent presented at the lowest snowfall accumulation height for convenience.

$S(K_{DP}, Z)$ computation adjusted for corresponding radar elevation. The range for the aspect ratios in aggregated snow is typically from 0.5–0.7 (Korolev and Isaac, [22]), and some recent studies (e.g. Garrett et al., [23]) advocate the use of b/a = 0.55. Garrett et al., [23] obtained this value with MASC system at the ground level.

Another notable feature in Fig. 4 is the "non-physical" slope of the total SWE estimated from $S(Z)$ relations. If saturation with respect to ice occurs below the DGL, all the way to the ground, then conservation of mass is preserved (in case of no advection below the DGL). As aggregation strengthens — Z increases (as a consequence of aggregation, the number of smaller anisotropic particles is deflated in the process and K_{DP} decreases). Thus, it is expected that total SWE estimated from $S(Z)$ have an almost constant profile from below the DGL and all the way to the ground because 80–90% of snow is produced in the DGL. In this case $S(Z)$s produce ~16, 19, and 25 mm at about 3 km AGL, which is ~50% of their total estimation at the ground level. On the other hand, both of $S(K_{DP}, Z)$ relations produce ~75–76% at ~ 3km AGL of their total amount at the ground level. Also, $S(K_{DP}, Z)$ relations' estimates of total SWE (Fig. 4: magenta and red line) are within ± 4–7% of reference ground measurement (55 mm), whereas $S(Z)$s underestimate total SWE by 42%, 31%, and 10% (Fig. 4: blue, green, and black lines, respectively). Clearly, $S(K_{DP}, Z)$ relations give physically more realistic profiles and more accurate total SWE amounts than the standard WSR-88D $S(Z)$ relations in this case.

b. 1 February 2011 case, Norman, Oklahoma

The 1 February 2011 snowstorm had a big impact on social life and it was highly disruptive. High snow accumulations on the ground (~30–50 cm, measured by the ruler) almost completely shut down northwestern parts of the state. Central Oklahoma saw 4–8 inches (about 10–20 cm) of snow depths on the ground. The measurements of total SWE in Norman were between 12 mm and 18 mm (determined from the storm snow depth reports and converted by 10:1 rule), about 15.3 mm on average, which is adopted as one of the ground reference measurements. The Norman Oklahoma Mesonet measurement of total SWE (few days after the storm, when snow melted) was ~ 12.9 mm.

The QVPs of Z, K_{DP}, Z_{DR}, and $S(K_{DP}, Z)$ presented in Fig. 5 show very interesting storm structure. There is a prominent bright band at about 1.8 km AGL, evident in Z and Z_{DR} enhancements from ~0300 until ~0845 UTC, but not as much in K_{DP} (most likely due to high elevation tilt of 19.5° used for QVP). There is also refreezing layer below the melting, as indicated by RUC model temperature profiles. The METAR reports (not shown) indicate that for the entirety of the event only snow was present on the ground, another independent confirmation of refreezing, which implies that some other type except the aggregated snow (perhaps rimed) could be present on the ground during that period. The enhancements in K_{DP} from 0300 to 1200 UTC (and also from ~1630 to 1700) are clearly visible in dendritic growth

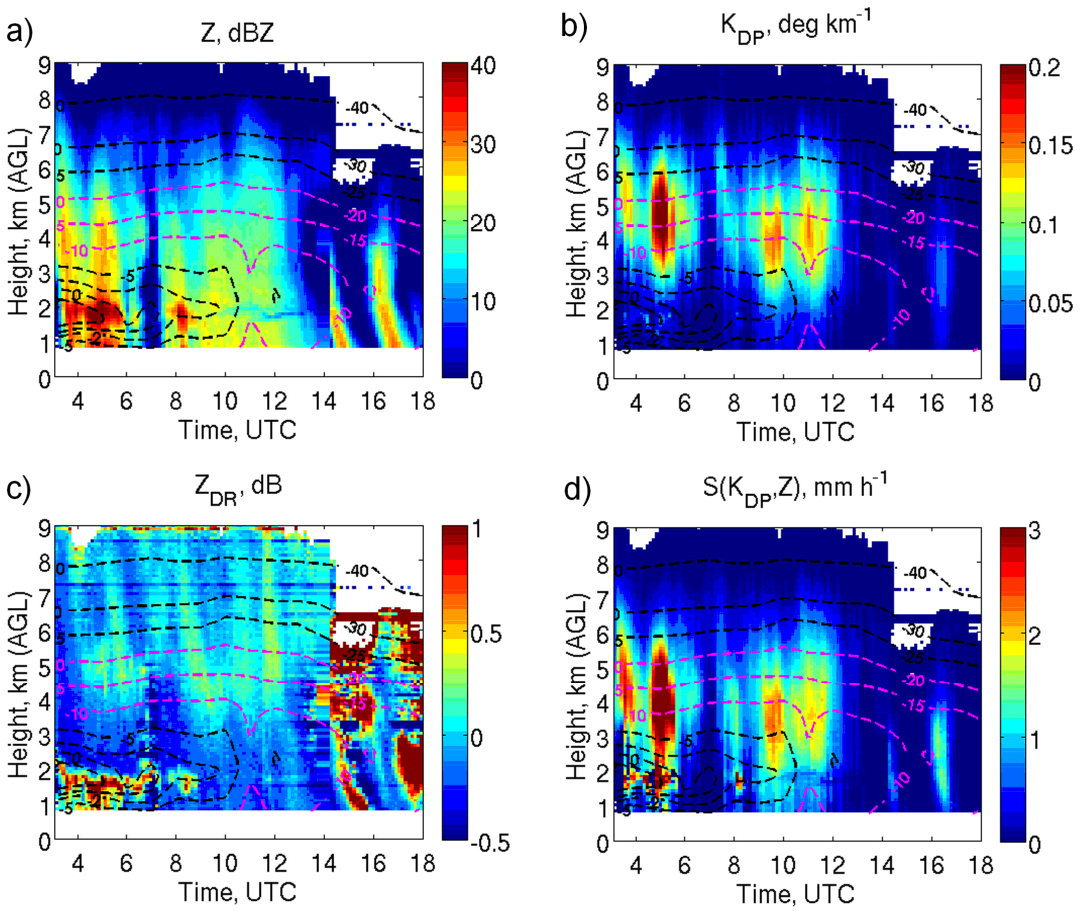

Figure 5. QVPs of a) Z in dBZ, b) K_{DP} in deg km^{-1}, c) Z_{DR} in dB, and d) S(K_{DP}, Z) in mm h^{-1}, KOUN 19.5° radar elevation angle, Norman OK, 1 February 2011. The black dashed lines are isotherms, where the layer from –10°C to –20°C highlighted in magenta represents DGL.

layer, between –10°C and –20°C. Another prominent feature in QVPs is localized moderate reduction in Z and slight enhancement in Z_{DR} (and also small reduction in co-polar correlation coefficient ρ_{hv}, not shown) at about 1.8 km AGL from ~0940 until 1340 UTC. This is an indication of the refreezing signature. The hypothesis is that partially melted particles from the melting layer may have been sustained at that level with the help of the wind shear and turbulence, which refroze as time progressed.

The QVPs of signal-to-noise ratio SNR (dB) and spectrum width SW (m s^{-1}) are shown in Fig. 6. There is a decrease in SNR from ~0930 to 1330 UTC at about 1.5 to 2 km height AGL, but values are well above 30 dB, making the associated signature in SW valid. The high values of SW at the edges of the echo are most likely associated with relatively low SNR but because of azimuthal averaging they are included in graphical representation. From the beginning of the event, the layer centered at ~1 km height AGL (it is bit higher at ~1.5 km height from 0930 until 1330 UTC) shows signs of moderate SW values (1.5 m s^{-1}), indicating the presence of wind shear and possibly turbulence. This is important because K_{DP} is lower in the wind sheared and turbulent air due to more random particle orientations, and is possibly reflected in reduction in total SWE profile below the DGL, obtained from $S(K_{DP}, Z)$ (see Fig. 7).

Comparisons between the three standard $S(Z)$ and two $S(K_{DP}, Z)$ estimates of total SWE, obtained from QVPs, along with the ground reference measurements are shown in Fig. 7. First, $S(K_{DP}, Z)$ estimates have primary maximums in DGL as opposed to $S(Z)$ relations (melting layer

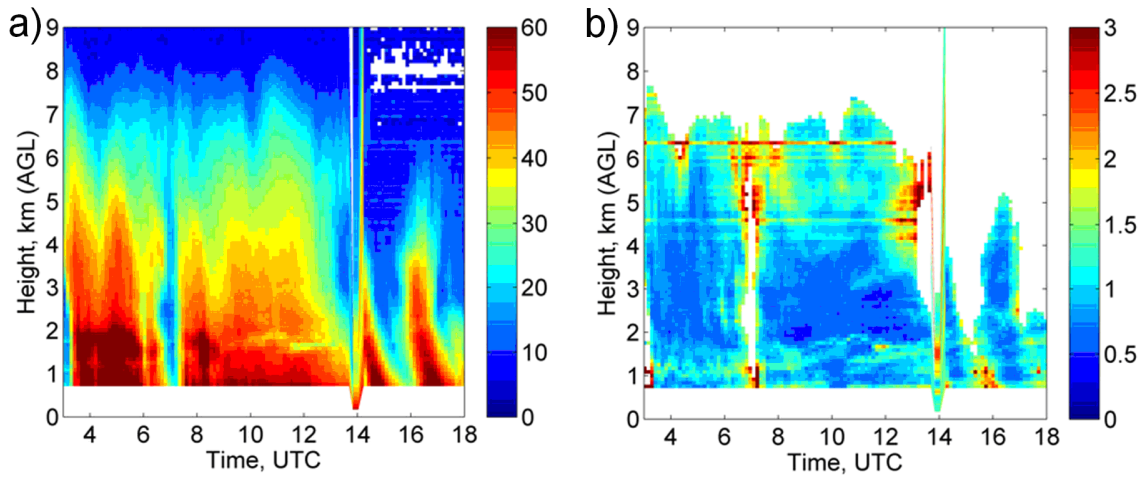

Figure 6. QVPs of a) SNR (dB) and b) spectrum width SW (m s^{-1}) from 19.5° elevation, KOUN, 1 February 2011. The threshold of 20 dB in SNR is applied to SW.

maxima). This is important if wind shear and turbulence is present because 80% to 90% of snow precipitation is formed in the DGL. The hypothesis that the $S(K_{DP}, Z)$ from DGL can be used for estimation of total SWE amount on the ground seems very plausible for this type of situation (wind shear and turbulence are mostly below the DGL). Although the total SWE profile amounts estimated from $S(K_{DP}, Z)$ are underestimated close to the ground (~5 mm), their estimates from DGL (12.6 to 14.2 mm) are in excellent agreement with the reference ground measurements (~13 to 15 mm). The $S(Z)$ relations display very unrealistic total SWE profiles due to inclusion of the melting layer. But some of the $S(Z)$s have total SWE estimates (~15.5 and 18 mm) at the lowest altitudes similar to the ground measurements, which in this case is rather fortuitous.

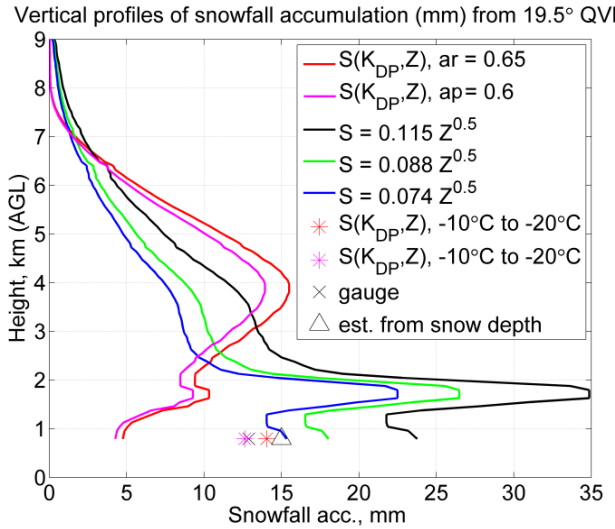

Figure 7. Vertical profiles of total snow liquid-water equivalent accumulation obtained from KOUN 19.5° QVPs using various $S(Z)$s and $S(K_{DP}, Z)$ relations (red: aspect ratio — ar = $(b/a)_{0°}$ = 0.65, magenta: apparent aspect ratio — ap = $(b/a)_{19.5°}$ = 0.6, obtained from $(b/a)_{0°}$ = 0.55 via Eq. 1) for 1 February 2011. The X represents reference ground measurements of snow liquid-water equivalent from Oklahoma Mesonet, whereas Δ is the estimate form the average snow depth measured by ruler across Norman, OK, using the 10:1 conversion rule, presented at the lowest snowfall accumulation height for convenience. Red and magenta asterisks are $S(K_{DP}, Z)$ estimates using aspect ratios of 0.65 and 0.6 respectively, but from DGL (–10°C to –20°C).

c. 28 January 2013 case, Grand Mesa, Colorado – Instantaneous snowfall rate verification

The winter precipitation measurement experiment, funded by Water Conservation Board of Colorado, was conducted in the vicinity of Grand Mesa, CO, from January until April 2013. The reduction

of the beam blockage effects from the 35°–40° azimuthal sector east of the KGJX WSR-88D radar, located in Grand Junction CO, was one of the primary goals of this experiment. This was the reason for the ground instrumentation placement in the middle of the beam blockage sector. Because the blockage affected the lowest radar elevations (0.5°, 0.9°), the next available (not affected) elevation (1.29°) is used for verification of $S(K_{DP}, Z)$ relations. The case presented had the largest snow accumulation (22.9 mm SWE) during the experiment period. The snow amounts were recorded with the heated rain gauge and 2DVD, located about 21 km east from the KGJX radar.

The instantaneous snowfall rate S obtained from 1.29° (450m AGL, 3500m MSL at the instrumentation location) scan is presented in Fig. 8. The data are computed as a median value of 5 range gates by 3° azimuth sector (median of 30 data points, about 1.2 km in diameter) extracted directly above the reference ground measurement location. The $S(K_{DP}, Z)$ relation used in this case is the one derived for the Colorado dataset, $S_{CO}(K_{DP}, Z) = 1.88\ K_{DP}^{0.61} Z^{0.34}$, as described in Bukovčić et al., [16], along with the standard $S(Z)$ relation of Vasiloff (1997) [24] which is tuned for this region. The relation $S_{CO}(K_{DP}, Z)$ follows more closely and consistently the ground reference measurement compared to $S(Z)$ relation. The only discrepancy occurred at the onset of the precipitation recorded with the heated gauge, from ~0400 to 0430 UTC, when $S(Z)$ produced values closer to the gauge measurements. In this period, there was moderate number of relatively large particles present, which $S_{CO}(K_{DP}, Z)$ couldn't properly address. At the end of the event, from 2200 to 2400 UTC, both $S_{CO}(K_{DP}, Z)$ and $S(Z)$ show some light precipitation, but there was no record from the gauge. The time lag could also be (partially) attributed to low temperatures which dropped below –10°C at this point. There are some discrepancies between the gauge and 2DVD measurements, but those are attributed to discretization and different temporal resolutions between the instruments. Overall, the $S_{CO}(K_{DP}, Z)$ estimate

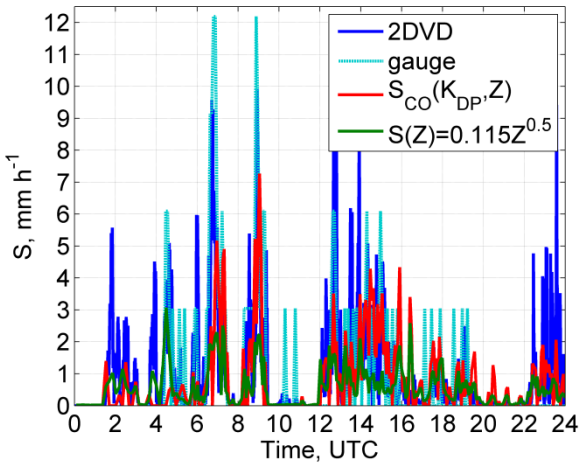

Figure 8. Instantaneous snowfall rate from heated rain gauge (dashed cyan line), 2DVD (blue line), $S_{CO}(K_{DP}, Z)$ (red line) and $S(Z)$ (green line) relations; 28 January 2013, Grand Mesa, CO.

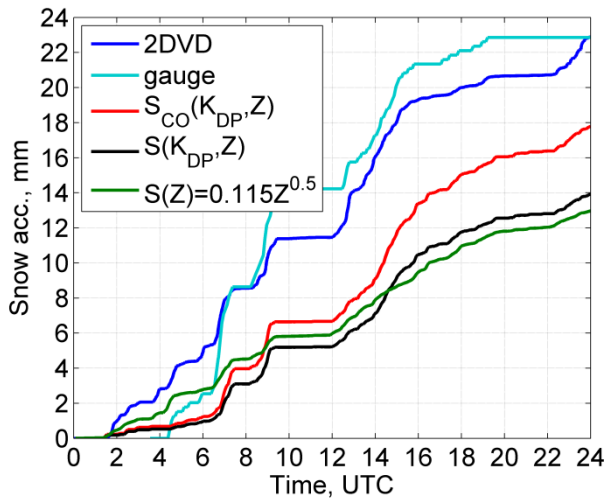

Figure 9. SWE accumulations from heated rain gauge (cyan line), 2DVD (blue line), $S_{CO}(K_{DP}, Z)$ (red line), $S(K_{DP}, Z)$ (black line), and $S(Z)$ (green line) relations; 28 January 2013, Grand Mesa, CO.

is more consistent with the 2DVD measurements than the $S(Z)$ relations' output.

Snow water equivalent accumulations from heated gauge, 2DVD, Colorado $S_{CO}(K_{DP}, Z)$, Oklahoma $S(K_{DP}, Z)$, and standard $S(Z)$ relations are presented in Fig. 9. Without taking into account the lagged gauge measurements, the $S_{CO}(K_{DP}, Z)$ relation produced the closest SWE amount (~18 mm) to the reference measurements (~22.9 mm), about 21% smaller. Also, the Okla-

homa $S(K_{DP}, Z)$ had closer values (~14 mm) than $S(Z)$ (~13 mm), ~39% and 43% smaller in comparison to the ground reference. The estimates from the $S(K_{DP}, Z)$s are in accord with the difference in the relations' multipliers, which is 21% higher for the Colorado relation. The shapes of both $S(K_{DP}, Z)$ curves resemble more the heated gauge, and especially 2DVD accumulations, than the $S(Z)$ counterparts. This is another example of the potentially universal character of the $S(K_{DP}, Z)$ relations, where the application to the radar data above the gauge location produced credible results.

5. Discussion

There are several sources of uncertainties in the polarimetric estimation of snowfall rate S. However, polarimetric relations are affected the most by the variations/changes in the particle density (degree of riming), snowflake shapes, and orientations. Polarimetric radar observations, in situ aircraft probes, and snow gauge measurements at the surface can help in assessment of these uncertainties. Hence the "adjustment" of proposed polarimetric relations, and more specifically their multipliers, could be obtained experimentally using the polarimetric radar data.

Analysis of the S-band K_{DP} measurements in heavily aggregated dry snow suggests that K_{DP} is usually noisy and very low. Due to its inverse proportionality to the wavelength, K_{DP} is higher at shorter radar wavelengths, i.e., at C and X bands. The corresponding relations at shorter wavelengths can be obtained by wavelength-scaling of K_{DP}.

The quality of radar snowfall measurements can be significantly improved if new polarimetric radar processing techniques, such as Quasi-Vertical Profiles (Ryzhkov et al., [19]; Griffin et al., [20]) and Enhanced/Column Vertical Profiles (Bukovčić et al., [18], Murphy [25]), are utilized. These techniques require substantial azimuthal/spatial averaging to reduce the statistical error of the K_{DP} estimate. Polarimetric measurements in the dendritic growth layer (DGL, temperature interval between -10°C and -20°C) suggest that the magnitude of K_{DP} within this layer is substantially higher than below the DGL, where warmer temperatures are expected (e.g., Kennedy and Rutledge, [26]; Bechini et al., [27]). These options should be further explored in future studies.

6. Summary

Verification of the polarimetric radar $S(K_{DP}, Z)$ relations in three geographical regions, Virginia, Oklahoma, and Colorado via reference ground measurements and comparison with the standard $S(Z)$ relations increase confidence in the applicability of the novel concept. Nonetheless, there are few issues with polarimetric measurements that need to be addressed. The most prominent ones are the dependence of the K_{DP} on snow density, and to somewhat higher extent the particle aspect ratio b/a and the width of the canting angle distribution σ. Specifically, the $S(K_{DP}, Z)$ relations' multipliers (γ) are strongly affected by these parameters' variation (snow density, b/a, and σ), whereas the relations' (K_{DP} and Z) exponents are almost invariant to these changes and can be regarded as constants. At the moment, the values of these parameters are obtained from the existing literature; the additional study is required to consolidate these estimates.

The use of the same $S(K_{DP}, Z)$ relation(s) in three distinct geographical regions (Virginia, Oklahoma, and Colorado) produced encouraging results, implying potentially universal character of these relations. There is an indication that if there is no presence of wind shear or turbulence, polarimetric relations produce more realistic profiles than the standard $S(Z)$ estimates. If turbulence and shear are present at lower levels (as indicated by spectrum width), more accurate estimates of S from $S(K_{DP}, Z)$ are obtained from the dendritic growth layer, where 80% to 90% of total precipitation is produced. The use of localized averaging on PPI data may produce adequate accuracy of K_{DP} (as shown in Colorado case) and increase the usability of polarimetric relations. In addition, in-

stantaneous snowfall rate from polarimetric relations obtained from PPI data in Colorado show better agreement with the ground measurements in comparison to the standard $S(Z)$ relation tuned for that region.

The estimates of K_{DP} are extremely noisy in aggregated snow and substantial spatial averaging may be required for its reliable estimation (Ryzhkov and Zrnic [12]). Hence, the usability of the novel polarimetric relations for snow measurements heavily depends on the K_{DP} accuracy. Extensive spatial averaging (as in QVP or CVP), and utilization of K_{DP} estimates aloft in the DGL (centered at the –15°C isotherm where the magnitude of K_{DP} is significantly higher than in heavily aggregated snow near the surface) or just above the freezing level, could significantly reduce the measurement error and noisiness in K_{DP}. Under the assumption that the mass flux is conserved, projection of the $S(K_{DP}, Z)$ values from dendritic growth layer to the ground should produce values in better agreement with ground measurements. Sensitivity of polarimetric relations to the temperature and relative humidity change are not directly taken into account in the present study, and should be a subject of a future research.

Acknowledgement

Special thanks are extended to Dr. Pengfei Zhang for QVP radar data processing and Dr. Guifu Zhang for the disdrometer data collection. This work is supported by NOAA/Office of Oceanic and Atmospheric Research under NOAA-University of Oklahoma Cooperative Agreement #NA16OAR4320115, U.S. Department of Commerce. Additional funding was provided through the NSF grant # 1841246.

References

1. *Gunn K.L.S.*, *Marshall J.S.* The distribution with size of aggregate snowflakes // Journal of Meteorology, 15, 1958. Pp. 452–461.

2. *Sekhon R.S.*, *Srivastava R.C.* Snow size spectra and radar reflectivity // Journal of the Atmospheric Sciences, 27, 1970. Pp. 299–307.

3. *Fujiyoshi Y.*, *Endoh T.*, *Yamada T.*, *Tsuboki K.*, *Tachibana Y.*, *Wakahama G.* Determination of a Z–R relationship for snowfall using a radar and sensitive snow gauges // Journal of Applied Meteorology and Climatology, 29, 1990. Pp.147–152.

4. *Matrosov S.* Modeling Backscatter Properties of Snowfall at Millimeter Wavelengths. / Journal of the Atmospheric Sciences, 64, 2007. Pp. 1727–1736. DOI: 10.1175/JAS3904.1.

5. *Matrosov S.Y.*, *Campbell C.*, *Kingsmill D.*, *Sukovich E.* Assessing snowfall rates from X-band radar reflectivity measurements // Journal of Atmospheric and Oceanic Technology, 26, 2009. Pp. 2324–2339.

6. *Szyrmer W.*, *Zawadzki I.* Snow studies. Part II: Average relationship between mass of snowflakes and their terminal fall velocity // Journal of Atmospheric and Oceanic Technology, 67, 2010. Pp. 3319–3335.

7. *Zhang G.*, *Luchs S.*, *Ryzhkov A.*, *Xue M.*, *Ryzhkova L.*, *Cao Q.* Winter precipitation microphysics characterized by polarimetric radar and video disdrometer observations in central Oklahoma // Journal of Applied Meteorology and Climatology 50, 2011. Pp. 1558–1570.

8. *Heymsfield A.*, *Matrosov S.*, *Wood N.* Toward Improving Ice Water Content and Snow-Rate Retrievals from Radars. Part I: X and W Bands, Emphasizing CloudSat // Journal of Applied Meteorology and Climatology. 55, 2016. Pp. 2063–2090, DOI: 10.1175/JAMC-D-15-0290.1.

9. *Vivekanandan J.*, *Bringi V.N.*, *Hagen M.*, *Meischner P.* Polarimetric radar studies of atmospheric ice particles // IEEE Transactions on Geoscience and Remote Sensing, 32, 1994. Pp. 1–10.

10. *Aydin K.*, *Tang C.* Estimation of ice water content with 94-GHz millimeter wave radar observables // Preprints, 27th Conf. on Radar Meteorology, Vail, CO, American Meteor Society, 1995. Pp. 550–552.

11. *Ryzhkov A.V.*, *Zrnic D.S.*, *Gordon B.A.* Polarimetric Method for Ice Water Content Determination / Journal of Applied Meteorology and Climatology, 37, 1998. Pp. 125–134. DOI: http://dx.doi.org/10.1175/15200450(1998)037<0125:PMFIWC>2.0.CO;2

12. *Ryzhkov A.*, *Bukovčić P.*, *Murphy A.*, *Zhang P.*, *McFarquhar G.* Ice microphysical retrievals using polarimetric radar data / In 10th European Conference on Radar in Meteorology and Hydrology, 1–6 July, Netherlands, 2018. Pp. 11. [Electronic source]. URL: https://projects.knmi.nl/erad2018/ERAD2018_extended_abstract_040.pdf (access date 14.01.2021).

13. *Lu Y.*, *Aydin K.*, *Cothiaux E.*, *Verlinde J.* Retrieving cloud ice water content using millimeter- and centimeter-wavelength radar polarimetric observables // Journal of Applied Meteorology and Climatology, 54, 2015. Pp. 596–604.

14. *Nguyen C.M.*, *Wolde M.*, *Baibakov K.*, *Korolev A.* Determination and estimation of high ice water content using X-band and W-band dual-polarization airborne radar data // In 38th Conference on Radar Meteorology, Chicago, IL, American Meteorological Society, 2017. P. 89.

15. *Nguyen C.M.*, *Wolde M.*, *Korolev A.* Determi-

nation of Ice Water Content (IWC) in tropical convective clouds from X-band dual-polarization airborne radar // Atmospheric Measurement Techniques, 12, 2019. Pp. 5897–5911.

16. *Bukovčić P.*, *Ryzhkov A.*, *Zrnić D.*, *Zhang G.* Polarimetric Radar Relations for Quantification of Snow Based on Disdrometer Data // Journal of Applied Meteorology and Climatology, 57, 2018. Pp. 103–120, DOI: 10.1175/JAMC-D-17-0090.1

17. *Ryzhkov A.*, *Zrnic D.* Radar Polarimetry for Weather Observations // Springer Atmospheric Sciences, 2019. 486 p.

18. *Bukovčić P.*, *Zrnić D.*, *Zhang G.* Winter Precipitation Liquid-Ice Phase Transitions Revealed With Polarimetric Radar and 2DVD Observations in Central Oklahoma // Journal of Applied Meteorology and Climatology, 56, 2017. Pp. 1345–1363. DOI: 10.1175/JAMC-D-16-0239.1

19. *Ryzhkov A.*, *Zhang P.*, *Reeves H.*, *Kumjian M.*, *Tschallener T.*, *Simmer C.*, *Troemel S.* Quasi-vertical profiles – a new way to look at polarimetric radar data // Journal of Atmospheric and Oceanic Technology, 33, 2016. Pp. 551–562.

20. *Griffin E.*, *Schuur T.*, *Ryzhkov A.* A polarimetric analysis of ice microphysical processes in snow, using quasi-vertical profiles // Journal of Applied Meteorology and Climatology, 57, 2018. Pp. 31–50. DOI: 10.1175/JAMC-D-17-0033.1

21. *Ryzhkov A.*, *Melnikov V.*, *Zrnic D.* Measurement errors of meteorological polarimetric radars and the ways to mitigate them // Радиотехнические и телекоммуникационные системы. №2. С.15– 25.

22. *Korolev A.*, *Isaac G.* Roundness and aspect ratio of particles in ice clouds // Journal of the Atmospheric Sciences, 60, 2003. Pp. 1795–1808.

23. *Garrett T.J.*, *Yuter S.E.*, *Fallgatter C.*, *Shkurko K.*, *Rhodes S.R.*, *Endries J.L.* Orientations and aspect ratios of falling snow // Geophysical Research Letters, 42, 2015. Pp. 4617–4622, DOI: 10.1002/2015GL064040

24. *Vasiloff S.* Interpretation of radar data during snow events in mountainous terrain // Western Region Technikal Attachment, 97-35, 1997, 16 p.

25. *Murphy A.* A Microphysical Analysis of the Stratiform Rain Region of Mesoscale Convective Systems using Polarimetric Radar and In Situ Aircraft Measurements // M.S. thesis, School of Meteorology, The University of Oklahoma, 2018. 124 p. [Electronic source]. URL: https://hdl.handle.net/11244/301727 (access date 14.01.2021).

26. *Kennedy P.*, *Rutledge S.* S-band dual-polarization radar observations of winter storms // Journal of Applied Meteorology and Climatology, 50, 2011. Pp. 844–858.

27. *Bechini, R.*, *Baldini L., Chandrasekar V.* Polarimetric radar observations in the ice region of precipitating clouds at C-band and X-band radar frequencies // Journal of Applied Meteorology and Climatology, 52, 2013. Pp. 1147–1169.

Поступила 15 января 2021 г.

English

POLARIMETRIC RADAR RELATIONS FOR SNOW ESTIMATION

Petar Bukovčić — PhD; Research Fellow, the Cooperative Institute for Mesoscale Meteorological Research[1], the University of Oklahoma[2], the National Severe Storm Research Laboratory[3].
E-mail: Petar.Bukovcic@noaa.gov

Alexander V. Ryzhkov — PhD; senior research scientist, the Cooperative Institute for Mesoscale Meteorological Research[1]; adjunct professor, University of Oklahoma[2].
E-mail: Alexander.Ryzhkov@noaa.gov

[1,2,3]*Address:* 120 David L Boren Blvd., Norman, Oklahoma, USA, 73072.

Abstract: In the recent study, Bukovčić et al. (2018) used a large dataset of snow measurements from 2D video disdrometer in central Oklahoma to derive bivariate power-law polarimetric relations for liquid-equivalent snowfall rate using specific differential phase K_{DP} and radar reflectivity Z, $S(K_{DP}, Z) = \gamma K_{DP}^{\alpha} Z^{\beta}$. Sensitivity analysis showed that the multiplier γ of the $S(K_{DP}, Z)$ relation is affected to the certain extent by the changes in the aspect ratio and the width of the canting angle distribution, whereas the exponents α and β are practically invariant to these variations. Polarimetric relations for snow quantification are applied to the polarimetric S-band data and evaluated at three locations, Oklahoma, Virginia, and Colorado. The use of polarimetric relations showed significant improvement in snow estimates, exhibiting a smaller bias in comparison to the traditional Z-based methods, suggesting a good promise for more dependable radar estimates of snow.

Keywords: precipitation measurements, polarimetric ratios, spectrum width, polarizing radar methods, enhanced/column vertical profiles.